Computer Simulation of Electrodynamic Screens for Mars Dust Mitigation

Jason R. Robison, Rajesh Sharma, Jing Zhang, Malay K. Mazumder
Dept of Systems Engineering & Dept of Applied Science
University of Arkansas at Little Rock
phone: (1) 501-569-8055
e-mail: jrrobison@ualr.edu

***Abstract*— The feasibility of using electrodynamic screens (EDS) for clearing solar panels in the dusty atmosphere of Mars has been established. Considerable research is in progress for this technology for future missions to Mars and the moon. We present here our work in progress in the development of three EDS computer simulations. (1) A 1-dimensional, probability-based simulation which takes into account applied voltage, frequency, electrode spacing, and particle charge-to-mass ratio, and is effective for simulating large numbers of particles. This simulation uses MATLAB's built-in random number generator and a simple iterative approach to simulate large numbers (100's) of particles. (2) A discrete-time, 2-dimensional, physics-based simulation which considers the above variables plus atmospheric density, gravity, and number of phases has also been developed. This physics-based program provides a simulation of motion for a small number (< 100) of particles on an EDS, but requires recalculating the electric field for every iteration. (3) A finite-element, 2-dimensional, physics-based simulation which computes the values for blocks of space above the EDS is under development. In this simulation the particles travel between these blocks taking a particular time based on their velocity. In this program the computing time is reduced by calculating the electric field only once. Electric field calculations generated by these EDS simulations will be compared with models generated using COMSOL software and findings from experimental data.**

I. INTRODUCTION

Photovoltaic Cells are the lifeblood of any extraterrestrial mission, manned or unmanned [1]. The primary source of solar power degradation on Mars is sedimentation of dust from the Martian atmosphere onto the Photovoltaic (PV) cells [2, 3]. This sedimentation occurs continuously, though it is most pronounced during and after the worldwide dust storms which blanket Mars every few years. Atmospheric dust poses a serious problem to manned and unmanned missions to Mars when it obscures the incident light on the PV panel, which lowers the power produced by the PV cells.

This obscuration occurs in two ways. The first is atmospheric obscuration in which dust particles in the Martian atmosphere disperse light high above the PV cell [2]. The second type of obscuration is deposition obscuration. This is caused by dust particles

which fall upon and accumulate on the PV cells [3]. This mechanism contributed to the ending of the Mars Pathfinder mission and now causes lower power production from the PV cells on the Mars Exploration Rovers – Spirit and Opportunity. This deposition obscuration has been substantially less on the highly mobile Mars Exploration Rovers (MER), but a stationary solar panel which is not exposed to the constant vibration while traversing the Martian surface would rely on the sporadic wind-bursts on the Martian surface to clear the PV cells

The Electrodynamic Screen (EDS) is one of the primary technologies currently being investigated by NASA for dust mitigation on Mars [3, 4]. The EDS consists of a series of parallel electrodes embedded in a transparent substrate. These electrodes are excited by a three-phase AC voltage (1000V±, 4-30Hz) [Fig.1] to produce a traveling electromagnetic wave. The two types of EDS currently being studied are the 2-phase and 3-phase designs. The 2-phase EDS sets up a standing wave which levitates the particles but does not effectively move them from the screen. The 3-phase EDS has proven more effective in dust removal as it produces a traveling wave between the electrodes. The particles on the surface of the EDS are levitated and propelled by the electromotive force produced by this traveling wave [4]. Printed circuit board (PCB) based, 3-phase EDS have been used extensively to demonstrate the capabilities of the EDS. They have been used as a stepping stone for optimizing the operation of the screens and have shown dust removal efficiency (DRE) of greater than 95%. The power consumption of the EDS varies depending on electrode spacing, operating voltage, and frequency, but can consume as little as 4 W/m^2. The EDS can operate continuously to remove dust particles as they fall, but often it is only necessary to run the EDS for 30 seconds to remove the dust particles. Thus, only 3.3 mWh/m^2 are required for a daily cleaning cycle.

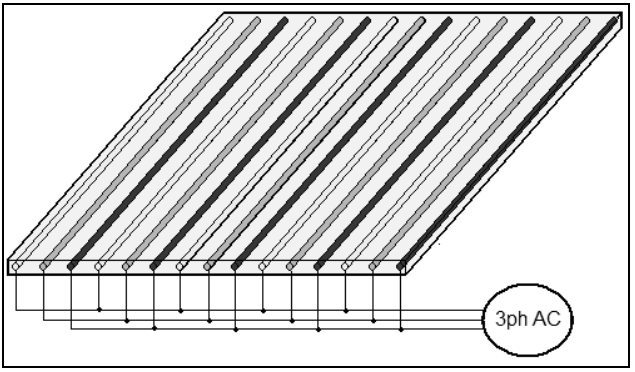

Fig.1: Illustration of 3-phase Electrodynamic Screen

II. BACKGROUND

Several research groups including NASA Jet Propulsion Laboratory, NASA Kennedy Space Center, and UALR have so far focused on optimizing the operation of EDS. Dust removal efficiency of EDS was increased by varying the parameters such as operating voltage, electrode spacing, electrode width, frequency, and run time, to find solutions

which are "close" to optimum [5, 6]. We are now developing computer simulations in parallel with these experiments to find the optimum parameters for maximizing dust removal efficiency of EDS.

Both analytical and computer simulation have been developed and verified for the 2-phase EDS [7], but not much work has been done with the 3-phase EDS. Thus, there is a need for development of a program for simulating particle motion on the 3-phase EDS. Previous computer simulation projects which considered electrostatic effects have proven effective at demonstrating the behavior of particles on the surface of the EDS. Initial findings show a great variety of responses to excitation waveforms and intensities.

III. Current Progress

This team is currently developing three simulations using MATLAB software. After the completion of the programming for these simulations is completed, the data will be verified not only with experimental results, but with COMSOL software known as FEMLAB. This software is one of the industry leaders in the field of Finite-Element Modeling (FEM).

A. Model (1): 1-D Probability Based Model

The first simulation presented uses a 1-dimensional, probability-based model which takes into account solely the charge/mass ratio of particles, but is highly efficient for modeling large numbers of particles. This model uses MATLAB's built-in random number generator and a simple iterative approach to model large numbers (100's) of particles. Outputs include graphics depicting the overall "flow" of positive, negative, and near-neutral particles based on current understandings of EDS function (Fig. 2). This model makes many assumptions about the factors contributing to the movement of particles. In this model the charge/mass ratio serves as a starting point for both the mean and the standard-deviation for the probability of particle movement. The Gaussian distribution

$$\tilde{x} = Gaussian(x) = \frac{1}{\sigma\sqrt{2\pi}} \exp\left(-\frac{(x-\mu)^2}{2\sigma^2} \right) \tag{1}$$

was chosen because it allows the movement in both positive and negative directions. The mean μ and standard-deviation σ were both based on the charge/mass ratio such that;

$$\mu = Q/M \cdot k_\mu : \sigma = Q/M \cdot k_\sigma \tag{2}$$

In this model k_μ and k_σ were chosen such that a desirable Probability Distribution Function (PDF) and realistic particle motion would be generated. In fig. 2.a, the values used for plotting the position vs. time, k_μ and k_σ, were 0.5 and 1.5 respectively, while Q/M was varied from -50 μC/mg to 50 μC/mg. In figure 2.b, the larger values of 5 and 2.5 were used to demonstrate the differences in the resulting PDF for three particles with positive (dashed), negative (dotted) and neutral (solid).

This model was the first stepping stone on the path to the more realistic models which are discussed later in this paper. This team is compiling data and results from these mod-

els, models generated with COMSOL simulation software, and most importantly with experimental data. The findings from these other sources will later be used to refine this model and to compare and test different theories in EDS design. This model will also allow for further EDS optimization based on results from other simulation and experimentation.

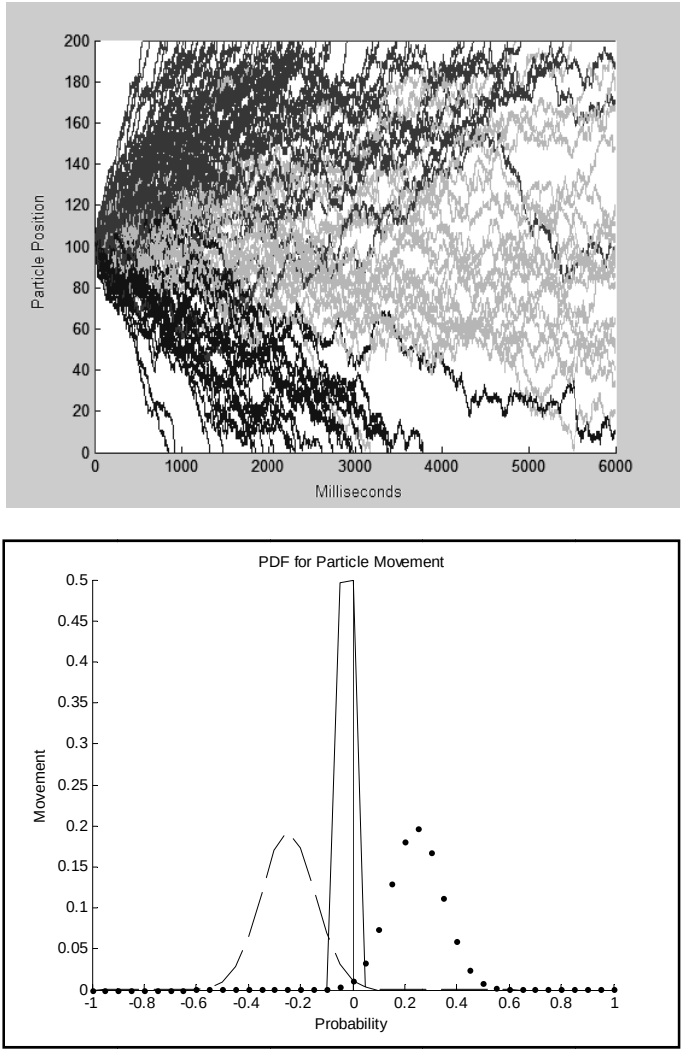

Fig.2: (a) Position Plot from 1-D model, (b) Gaussian Distribution for Particles with Given Charge

B. Model (2): 2-D Discrete-Time Physical Model

The next model presented is the discrete-time, 2-dimensional, physics-based model. This model considers charge/mass ratio Q/M, as well as atmospheric density ρ_{atm}, local

gravity g, electrode depth in substrate d_{elec}, particle density ρ_{part}, particles surface roughness C_d, number of phases n_ϕ, and phase voltage V_ϕ. This first attempt at a physics-based model provides simulation of motion for an individual particle on an EDS (Fig.2, 3). This model also uses an iterative approach to simulate particle motion. The model uses an orthogonal coordinate system such that: x is along the EDS surface, perpendicular to the electrodes; y is along the EDS surface, parallel to the electrodes; z is normal to the EDS surface. Only two dimensions are measured with this model, x and z. The EDS electrodes are considered to be infinite line charges along *y*, located at $z = -d_{coat}$, and $x = n \cdot d_{elec}$. The linear charge density for each electrode is calculated by using Gauss's Law to find the electric field for an infinite line charge.

$$\Phi = 2\pi r L \cdot E = \frac{\lambda L}{\varepsilon_0} \tag{3}$$

$$\mathbf{E} = \frac{\lambda}{2\pi r \varepsilon_0}\hat{\mathbf{r}} : V_{ab} = Er \tag{4}$$

This equation is then solved for linear charge density λ to produce the following equation.

$$\lambda = 2\pi\varepsilon_0 Er = 2\pi\varepsilon_0 V_{ab} \tag{5}$$

Thus, the sum of contribution for each input voltage applied at each of k given electrodes located at positions x_k can be found for a particular point in space given by x and z.

$$E_x = \sum_k \cos(\theta_k)\frac{\lambda_k}{2\pi\varepsilon_0 r_k} = \sum_k \frac{\lambda_k (x_k - x)}{2\pi\varepsilon_0 r_k^{\,2}} \tag{6}$$

$$E_z = \sum_k \cos(\theta_k)\frac{\lambda_k}{2\pi\varepsilon_0 r_k} = \sum_k \frac{\lambda_k (d_{elec} - z)}{2\pi\varepsilon_0 r_k^{\,2}} \tag{7}$$

This operation is done for each particle location during each iteration of the simulation using a sampling time T_s.

A weak point of this model is found as a particle begins traveling very fast. As the particle moves through a fluctuation in the electric field, it travels farther and farther before the next iteration occurs. This results in the particle moving faster than the actual motion, resulting in greater inaccuracies. Another undesirable aspect of this model is its long computation time. This model requires the calculation of the electric field produced by each electrode at the position of each particle during each iteration. As the number of electrodes k, particles N_p, or iterations N_{iter} increases, the total number of contribution calculation cycles N_{cycle} increases.

$$N_{cycle} = k \cdot N_p \cdot N_{iter} \tag{8}$$

This makes the model difficult to operate for a larger number of particles, electrodes, or time divisions. Forces considered include electromotive force, aerodynamic drag force, and gravitational force.

The position plot of a single particle (Fig: 3.a) shows simulated motion above a 3-phase EDS. The particle oscillates for approximately $3s$ before it begins moving along with the travelling electric wave. The velocity plot of a single particle (Fig: 3.b) is equally interesting, showing gradual "curved" changes in velocity from the action of the varying electric field above the EDS as well as sudden jumps from negative to positive velocity. The latter feature correlates with the particle making contact with the EDS surface and bouncing off.

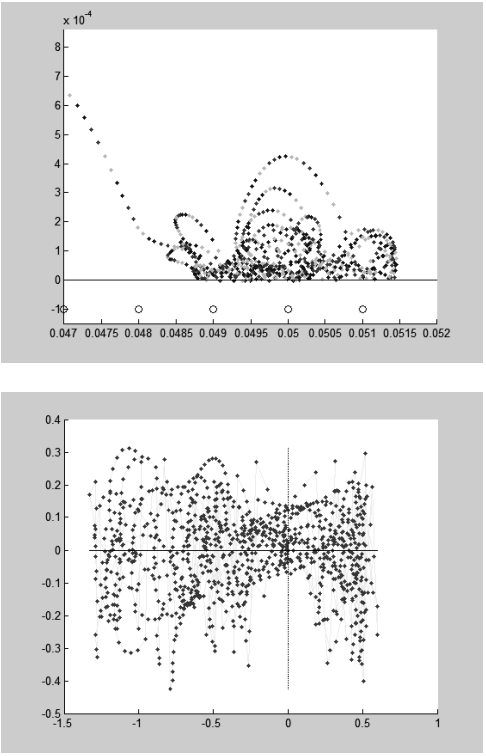

Fig.3: (a) Position Plot from 2-D DT Model, (b) Velocity Plot from 2-D DT Model.

C. Model (3): 2-D Finite-Element Physical Model

The final model presented is a finite-element, 2-dimensional, physics-based model which computes the values for blocks of space above the EDS (Fig.4). In this simulation the travel of the particle between these blocks taking a particular time period based on their velocity. Each particle has an update time on a "calendar", and when the update time for

a given particle is reached; the electric field intensity is then re-evaluated at the new location. In this model the computing time is reduced by calculating the electric field only once at the beginning of the simulation, and then updating particle velocity each time it passed into a new block. This more advanced algorithm should remedy both problems faced by the discrete-time model.

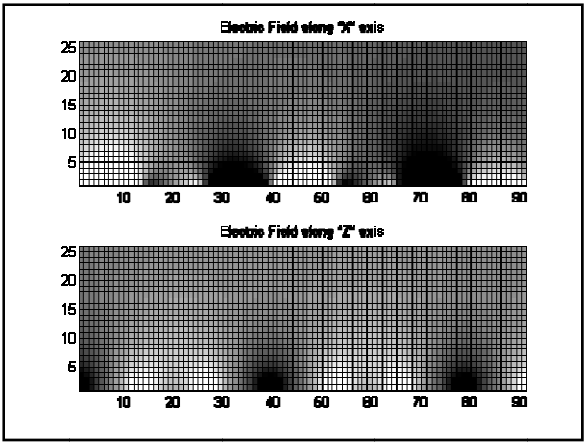

Fig.4: Electric Field above an EDS; Darker areas represent Negative Field, Lighter represents Positive.

There are several difficulties faced when using this method. The first being the method of translating the direction of particle velocity into the orthogonal measurement system mentioned in the previous paragraphs.

1) Strictly Orthogonal Velocity

One option is to allow movement only along the two axes, x and z. This method is the simplest, but provides the most opportunity for inaccuracy in the model. When the ratio of x to z is considered, the following can be seen.

$$\frac{|V_X|}{|V_Z|} > 1 : \text{Along X} \qquad \frac{|V_X|}{|V_Z|} < 1 : \text{Along Z} \tag{9}$$

The simulated movement will be least accurate with constant angle of velocity with nearly equal V_X and V_Z components (Fig.5).

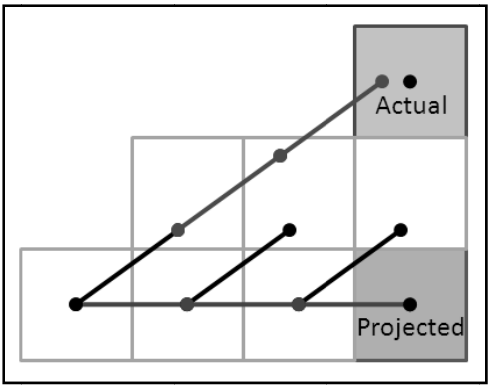

Fig.5: Illustration of Inaccuracy due to Strictly Orthogonal Movement

2) Orthogonal and Diagonal Velocity

The next method uses both orthogonal and diagonal movement. This results in a more complex algorithm, but reduces the maximum error in angle roughly by half. This is because the number of available directions is doubled.

$$\text{ò}_{Max,4} = \frac{\pi}{4} \qquad \text{ò}_{Max,8} = \frac{\pi}{8} \tag{10}$$

One of the complexities is the necessity for predicting the arrival time of the particle when the exact distance travelled will vary depending on direction traveled. The distance traveled when a particle moves between orthogonally adjacent blocks d_{Ortho} is based on the resolution of the simulation and the distance between electrodes, whereas the distance moved between diagonally adjacent blocks d_{Diag} is $\sqrt{2}$ times greater.

$$d_{Ortho} = d_{(i,i\pm1)} = d_{(j,j\pm1)} = \frac{d_{elec.}}{res} = l \qquad d_{Diag} = d_{(j,j\pm1|i,i\pm1)} = \sqrt{\left(d_{(i,i\pm1)}\right)^2 + \left(d_{(j,j\pm1)}\right)^2} = l\sqrt{2} \tag{11}$$

This complexity is compounded when determining which block the particle will travel to next, based on the particle velocity and distance between blocks. One method of determining the next location could be to use a probability based algorithm, but this would require more computer time to accomplish. It can be shown that the angle at which the probability being equal for the particle to enter either block passes through the midpoint of the contiguous border of those blocks (Fig.6). This angle can be found by comparing the x and z distances travelled.

$$\theta_{crit} = \tan^{-1}\left(\frac{1}{2}\right) = 26.6° \tag{12}$$

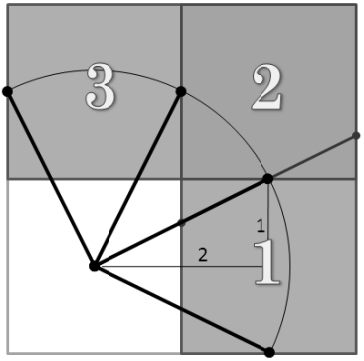

Fig.6: Illustration of Target Determination for varying Velocity Angles

The critical angle can be found by taking the inverse tangent, and the critical angle for each of the orthogonal directions of travel θ_{Ortho} can be found from the following.

$$\theta_{Ortho} = 90°n \pm 26.6° : n = 1,2,3,4 \tag{13}$$

The remaining diagonal directions θ_{Diag} can be found from this equation.

$$\theta_{Diag} = 45° + 90°n \pm (45° - 26.6°) = 90°(n + 1/2) \pm 18.4° : n = 1,2,3,4 \tag{14}$$

It can be speculated that the ratio of angles assigned to θ_{Diag} to those assigned to θ_{Ortho} should vary inversely with the distances between blocks.

$$\frac{d_{Ortho}}{d_{Diag}} = \frac{l}{l\sqrt{2}} = 0.71 \qquad \frac{\theta_{Diag}}{\theta_{Orhto}} = \frac{26.6°}{18.4°} = 0.69 \tag{15}$$

This requires making the assumption that the probability of movement into a given block decreases linearly with distance, an assumption which has not been tested.

IV. Future Work

The next goal of this project is to continue the development of the finite-element 2-dimensional model and incorporate several other variables including: particle resistivity, inter-particle collisions, and inter-particle charge transfer. Experimentation will be conducted to verify the particle dynamics of the MATLAB model. These will include en-masse particle removal with respect to time to verify particle removal, and collection of particles using a Faraday cup to verify particle charge characteristics. Other possibilities include advanced particle-racking techniques such as E-SPART [8] or LDV [9]. E-SPART technology could be used to check the simulated flow of particles in a given direction. LDV technology could be used to verify particle speeds during certain phase

increments and at certain distances above the EDS. After reviewing this data, the models will be refined to better simulate EDS operation.

REFERENCES

[1] Gaier, J. R., R. A. Creel, et.al. (2005). "The Effects Of Lunar Dust on Advanced EVA Systems: Lessons Learned from Apollo."

[2] Pollack, J.B., Colburn, D.S., et.al. (1979) "Properties and effects of dust particles suspended in the martian atmosphere." J. Geophys. Res.; Vol 84: IssueB6: 2929-2946.

[3] Landis, G.A. (1997), "Mars dust removal technology." Energy Conversion Engineering Conference, 1997. IECEC-97.;Vol: 1, 764-767.

[4] Mazumder, M. K., Sharma. R., et al. (2007). "Self-Cleaning Transparent Dust Shields for Protecting Solar Panels and Other Devices." Particulate Science and Technology, 25: 5–20, 2007.

[5] Immer, C., J. Stares, et.al. (2006). "Electrostatic Screen for Transport of Martian and Lunar Regolith." Lunar and Planetary Science XXXVII, 2006: 2265-2266.

[6] Wyatt, C., Sharma. R., et.al (2007) "Development of flexible electrodynamic screen for lunar dust mitigation on EVA suits and exploration equipment." Proceedings of the ESA Annual Meeting on Electrostatics 2007: 250-258.

[7] Chen, A., Meyer J., et.al. (2006) "Numerical and analytical model of an electrodynamic dust shield for solar panels on Mars." Lunar and Planetary Science XXXVII, 2006: 1873-1874.

[8] Srirama , P.K.; Mazumder, M.K. (2004), "Measurement of charge distribution of highly charged particles by E-SPART analyzer." Conference Record of the 2004 IEEEIndustry Applications Conference, 2004. 39th IAS Annual Meeting, 2004. Vol: 2: 1280 -1282.

[9] Biittner, L., Czarske, J. (2004), "Laser Doppler velocity profile sensor using a two-wavelength technique and diffractive optics." Conference on Lasers and Electro-Optics(CLEO), 2004. Vol: 1.